HHS Public Access

Author manuscript

Gene Ther. Author manuscript; available in PMC 2019 November 24.

Published in final edited form as:

Gene Ther. 2019 June ; 26(6): 277–286. doi:10.1038/s41434-019-0080-9.

Feasibility of Using NF1-GRD and AAV for Gene Replacement Therapy in NF1-Associated Tumors

Ren-Yuan Bai, **Dominic Esposito**[2], **Ada J. Tam**[3], **Frank McCormick**[2], **Gregory J. Riggins**, **D. Wade Clapp**[4], and **Verena Staedtke**[1]

[1]Department of Neurosurgery and Neurology, Johns Hopkins University School of Medicine, Baltimore, MD, USA.

[2]NCI RAS Initiative, Frederick National Laboratory for Cancer Research, Leidos Biomedical Research, Inc., Frederick, MD 21701.

[3]Bloomberg-Kimmel Institute for Cancer Immunotherapy, Johns Hopkins University School of Medicine, Baltimore, MD, USA.

[4]Department of Pediatrics, Indiana University School of Medicine.

Abstract

Neurofibromatosis type 1, including the highly aggressive malignant peripheral nerve sheath tumors (MPNSTs), is featured by the loss of functional neurofibromin 1 (NF1) protein resulting from genetic alterations. A major function of NF1 is suppressing Ras activities, which is conveyed by an intrinsic GTPase-activating protein-related domain (GRD). In this study, we explored the feasibility of restoring Ras GTPase via exogenous expression of various GRD constructs via gene delivery using a panel of adeno-associated virus (AAV) vectors in MPNST and human Schwann cells (HSC). We demonstrated that several AAV serotypes achieved favorable transduction efficacies in those cells and a membrane-targeting GRD fused with an H-Ras C-terminal motif (C10) dramatically inhibited the Ras pathway and MPNST cells in a NF1-specific manner. Our results opened up a venue of gene replacement therapy in NF1-related tumors.

Keywords

NF1; MPNST; AAV; GRD; Gene Replacement; Ras

Introduction

The RASopathy neurofibromatosis 1 is an autosomal dominant hereditary cancer syndrome that affects ~1:3,000 individuals [1, 2]. Neurofibromatosis 1 is caused by mutations of the *neurofibromin 1 (NF1)* tumor suppressor gene at 17q11.2, which encodes the GTPase-

Corresponding Authors: Ren-Yuan Bai or Verena Staedtke, Johns Hopkins University, Koch Building Rm. 245 or Rm 1M43, 1550 Orleans Street, Baltimore, MD 21231, Phone: 410-614-6550; Fax: 410-502-5559, rbai1@jhmi.edu or vstaedt1@jhmi.edu.

Conflict of Interest: A provisional patent application on Rasopathy treatment listing R.Y.B. and V.S. as co-inventors was filed by JHU.

activating protein (GAP) NF1 that catalyzes the inactivation of Ras by accelerating GTP hydrolysis to GDP [3, 4]. In affected individuals, truncation or loss of *NF1* results in constitutively activated Ras with subsequent activation of the RAF–MEK–ERK cascade. This Ras hyperactivation supports the frequent development of multiple benign tumors, as in plexiform and cutaneous neurofibromas, and less frequently malignancies.

A hallmark of neurofibromatosis 1 is the presence of benign plexiform neurofibromas (pNFs) in which biallelic-inactivating mutations in the *NF1* gene in Schwann cells occur and provides a selective growth advantage to a normal Schwann cell [2, 5]. About 8–13% of pNFs undergo cancerous transformation into a malignant peripheral nerve sheath tumor (MPNST) through a course of molecular evolution during which accumulated genetic mutations in *CDKN2A/B*, *TP53* and other genes as well as epigenetic alternations affect the regulation of multiple cellular processes [2, 6]. This transformation evolves over many years and typically affects young adults with neurofibromatosis 1 in their 20s-30s, with MPNSTs representing the leading cause of mortality in this patient population [7, 8].

The treatment of MPNSTs has unfortunately been extremely challenging. To date, surgery is the only treatment modality proven to have survival benefit for MPNSTs. However, even when maximal surgery with wide surgical margins is feasible, these tumors are almost never curable [8, 9] and about 50% of patients will succumb to this condition within 5 years after initial diagnosis, reflecting the urgent need for new and more effective therapeutics for this cancer.

One very promising but largely unexplored concept in the treatment of NF1-related MPNSTs is gene therapy. Over the past years, delivery vectors based on recombinant adeno-associated virus (AAVs) have shown great promise and achieved clinically meaningful long-term gene expression leading to regulatory approval for some conditions such as hemophilia, cystic fibrosis and spinal muscular atrophy (SMA) [10–12].

The recombinant AAV is a non-pathogenic, non-replicating parvovirus because *rep* and *cap* genes are cloned in a trans-plasmid without inverted terminal repeats (ITR). To date more than 100 natural occurring human and non-human primate AAV serotypes have been identified [13]. Unlike lentivirus, it does not cause any human disease and has a reduced carcinogenicity because it only rarely integrates into the genome of the host cell. It is capable of infecting both dividing and quiescent cells with a low host immune recognition. Notably, advancements in our understanding of AAV capsid structure have facilitated the rational design of AAV capsids to restrict or redirect viral tropism and transduction, and considerable progress in both AAV capsid library development and screening methodology has enabled directed evolution of AAV capsids, which will ultimately ensure that transgene expression is reproducible, robust, and occurs over an extended period [13–15].

Gene delivery vectors based on AAVs have a packaging capacity of up to ~4.7 kb at near wild-type titers and infectivity; beyond this size, packaging efficiency markedly decreases, and genomes with 5′ truncations become encapsidated [14]. Although *NF1*'s cDNA of 8.5 kb is too large for AAV vectors, the NF1-GAP-related domain (NF1-GRD), a ~1kB small

subunit of the gene, is presumably solely responsible for deactivating Ras activity [16, 17] and, thus making neurofibromatosis 1 uniquely suitable for AAV based gene delivery.

In this study, we have screened a panel of available AAV vectors in MPNST and primary Schwann cells to profile transduction efficacies of different serotypes in order to reveal potential templates for future engineering of the AAV capsid. We also tested the inhibition of the Ras pathway in NF1-related MPNST cells using GRD optimized for membrane-targeting.

Materials and Methods

Tissue culture and cell lines

Human NF1-associated MPNST cell lines NF90.8 and ST88–14 were provided by Dr. Michael Tainsky (Wayne University, Detroit, MI) and sNF96.2 was purchased from ATCC (Manassas, VA). NF90–8, ST88–14, sNF96.2 and STS26T MPNST cell lines were cultured in DMEM (ATCC) media supplemented with 10% FBS (Sigma) and penicillin/streptomycin (Gibco). These cell lines were not authenticated. Human Schwann cells isolated from spinal nerve were purchased from ScienCell Research Laboratories and maintained in DMEM media supplemented with 3% FBS, penicillin/streptomycin, and heregulin-1 (PeproTech) 20 ng/ml and 2 μM forskolin (Sigma). All cells were tested and found free of mycoplasma contamination.

Reagents and antibodies

The rabbit anti-phospho-Erk1/2 (p44/42 MAPK) (Thr202/Tyr204) antibody (#9101, Lot 23) and anti-Erk1/2 (p44/42 MAPK) antibody (#9102, Lot 27) were purchased from Cell Signaling Technologies. Rabbit anti-NF1 antibody (A300–140A, Lot 3) was purchased from Bethyl laboratories, mouse anit-HA antibody (26183, Lot RJ241582) was purchased from Invitrogen and anti-βActin (C-11, SC-1615HRP, Lot G3015) HRP antibody was purchased from Santa Cruz Biotech. Active Ras Detection Kit (#8821, antibody Lot 7) was purchased from Cell Signaling Technology. NucBlue Live Ready Probes was purchased from Invitrogen.

NF1-GRD constructs

Human NF1 transcript variant 2 (NM_000267.3) of 2818 amino acids (AA) was used as the template sequence. The GRD sequence of NF1 (AA 1172–1538) as described before [18], was cloned with a C-terminal 2xHA tag into the lentivirus pFUGW and pscAAV-MCS (Cell Biolabs, VPK-430) vectors. To create a membrane-targeting GRD construct (GRD-C10), a 2xHA sequence was fused to the N-terminus of GRD and a sequence encoding the H-Ras C-terminal 10 AA (GCMSCKCVLS) containing the CAAX motif was attached in frame to the GRD C-terminus.

Lentiviral production and transduction

EGFP or GRD-2HA was cloned in pFUGW vector and the plasmid was transfected along with CMVΔR8.91 and pMD.G in 293T cells by Lipofectamine 2000 (Invitrogen). Virus was

harvested after 48 hours and infected MPNST cells by incubating with 8 μg/ml polybrene (Sigma).

AAV plasmids

pscAAV was purchased from Cell Biolabs, Inc. We obtained 13 hybrid pAAV-Rep-Cap (pAAV-RC) vectors, which encode the rep of AAV2 and variable *cap* genes of different serotypes. Among them, pAAV2-RC was purchased from Stratagene, pAAV-RC3B, pAAV-RC4, pAAV-RC6 and pAAV-DJ were purchased from Cell Biolabs, and pAAV2/1, pAAV2/5 JC, pAAV2/7, pAAV2/8, pAAV9n, pAAV2/rh10, pAAV2/hu11 and pAAV2/rh32.33 were obtained from Penn Vector Core of the University of Pennsylvania. For AAV packaging, the pHelper plasmid (Stratagene) and AAVpro-293T cells (Clontech) were used.

AAV production and purification

pAAV-Rep-Cap, pscAAV and pHelper plasmids in equal amount were transfected in AAVpro-293T cells by Lipofectamine 2000 in DMEM media supplemented with 10% FBS. After 3 days, cells were harvested and AAVs were purified by AAVpro Purification Kit of Clontech following the manufacturer's instruction. Viral titers were determined by AAVpro Titration Kit from Clontech using real-time PCR.

AAV transduction and fluorescence microscopy

In a flat bottomed 96 well plate, 5000 of HSC or MPNST cells were plated in each well. AAV vectors with EGFP were incubated at MOI 1000 or MOI 5000 in 60 μl in the regular growth media for 5 days. Medium was then changed to FreeStyle 293 Expression medium (Gibco) without Phenol Red added with NucBlue Live Cell Stain ReadyProbes (Invitrogen) that stained the nuclei to blue fluorescence. The cells have reached complete confluence and the green fluorescence signals were quantified on a PerkinElmer VICTOR3 1420 Multilabel Counter with a green fluorescence (485/535 nm) filter set. EGFP signals were subsequently examined on an immunofluorescence microscope. Three biological samples were measured in each experiment.

Immunofluorescence Staining

The staining followed the procedure described before [19]. Cells were grown in medium on chamber slides (Nunc) and treated as indicated. Cells were washed with PBS and fixed for 10 min with 4% paraformaldehyde solution and permeated with methanol for 2 min with 3 washes in PBS in between and after. The slides were first blocked by 10% goat serum in PBS for 1 h at room temperature and incubated with the first antibody and subsequently with AlexaFluor 488 (Green) secondary antibody (Invitrogen) in 10% goat serum in PBS at room temperature. They were then washed 3 times in PBS in between and after. After staining, the slides were covered with mounting medium containing DAPI (Vector Laboratories) and examined on a fluorescence microscope.

Western Blots

Cells were lysed in buffer as described previously [20] [19]. Briefly, cells were suspended in lysis buffer (10 mM Tris-HCl pH 7.5, 130 mM NaCl, 5 mM EDTA, 0.5% Triton X-100, 20

mM sodium phosphate pH 7.5, 10 mM sodium pyrophosphate pH 7.0, 50 mM NaF, 1 mM sodium orthovanadate,1 mM phenylmethylsulfonyl fluoride, and protease inhibitor cocktail [Roche]) and kept on ice for 10 min before being centrifuged. Cell lysates were heated for 5 min with LDS Sample Buffer (Invitrogen) supplemented with 100 mM DTT before loading onto a 4–12% NuPAGE Bis-Tris Gel (Invitrogen). After transfer to a PVDF membrane (Bio-Rad), immunostaining was performed according to standard procedure. Signals were visualized by the Super Signal chemiluminescent system (Pierce, Rockford, IL). Experiments were repeated twice.

Assay of active Ras

Ras activities in MPNST cells were examined by the Active Ras Detection Kit (#8821, Cell Signaling Technology) following manufacturer's instuction. Briefly, the cell lysates were incubated with GST-Raf1-RBD and glutathione resin. After wash and centrifugation, the bound fractions of Ras were dissociate and denatured in SDS sample buffer with DTT, and examined by anti-Ras western blotting. Pre-incubating the lysates with 0.1 mM GTPγS or 1 mM GDP before binding with GST-Raf1-RBD created positive or negative control, respectively. Experiments were repeated twice.

Cell Growth Assay

The viable cells were measured with Cell Counting Kit-8 (Dojindo Laboratories, Japan) containing WST-8 tetrazolium salt at 450 nm on a PerkinElmer VICTOR3 plate reader. Three biological samples were measured in each experiment.

Flow Cytometry

Analysis of EGFP-positive cells—NF90–8 cells in6-well plates were incubated with AAV-DJ-EGFP at MOI 1000 or 5000 for 36 hrs. Cells were harvested by trypsinization, counterstained by incubating with 28 mM DAPI for 5 min in the flow buffer (PBS with 4% FBS and 1 mM EDTA), washed and analyzed by a BD FACSAria Fusion at the FITC channel. Control was untransfected cells. Three independent samples were measured and data were analyzed by two-tailed t-test.

Staining of GRD-2HA and GRD-C10–2HA transfected by AAV-DJ—NF90–8 cells in 6-well plates were incubated with AAV-DJ control, AAV-DJ-GRD-2HA or AAV-DJ-GRD-C10–2HA at MOI 5000 for 36 hrs. Cells were trypsinized, fixated by the IC fixation buffer (Invitrogen, #00–8222), permeabilized by the permeabilization buffer (Invitrogen, #00–8333) and incubated with anti-HA antibody conjugated with AlexaFluor 647 (R&D Systems, #IC6875R) at 5 μl/ 10^6 cells in 100 μl permeabilization buffer for 45 min at RT. Cells were then washed twice in 2 ml permeabilization buffer, resuspended in 0.5 ml flow buffer and analyzed by a BD FACSAria Fusion. Data were obtained from three independent samples and analyzed by two-tailed t-test.

Propidium Iodide (PI) Staining—Cells were plated in 6-well plates and transduced with indicated AAVs. After 2 days, cells were trypsinized, washed, pelleted and fixated with 70% ethanol at the final concentration on ice for 15 min. Cells were then centrifuged and incubated with 500 μl PI-solution in PBS (50 μg/ml PI, 0.1 mg/ml RNase A, 0.05% Tritin

X-100) at 37°C for 40 min. Subsequently, cells were washed and resuspended in PBS and analyzed with a BD FACSymphony A3 flow cytometer using the PE-Gr-A channel. Results were analyzed with FlowJo version 10.

Statistical Analysis

The results are presented as a mean value plus or minus the standard deviation. Data were analyzed by GraphPad Prism 5.0. The p-values were determined by a Mantel-Cox test. A p-value under 0.05 was accepted as statistically significant. Sample sizes were chosen to achieve statistical significance.

Results

1. NF1-GRD suppressed the RAS activity and the growth of MPNST cells

Expressing the GRD domain of NF1 could restore normal growth in NF1−/− NF1-deficient hematopoietic cells, fibroblasts and neural stem cells [16, 17]. Likewise, the effects of the GRD have also been demonstrated in MPNST cells [21, 22].

In this study, we first subcloned the GRD domain of human NF1 into the pFUGW lentivirus (LV) vector with a C-terminal double HA tag (2HA) for sensitive in vitro and in vivo detection. Human MPNST cells NF90.8, sNF96.2 and ST88–14 were derived from patients with neurofibromatosis 1 and lacked the wildtype (WT) *NF1* gene, whereas both STS26T cells derived from a sporadic MPNST and primary human Schwann cells isolated from spinal nerve expressed functional *NF1* [23]. Figure 1A confirmed the expression status of NF1 protein in these cells. As shown in Figure 1B, the GRD-2HA construct was able to significantly reduce the aberrant Ras activity in ST88–14 and NF90.8 cells in the GST-Raf1-RBD pulldown assay suggesting that the GAP domain of NF1 compliments the inability of these cells to inactivate RAS. The replacement of the NF1-GRD via lentiviral transduction significantly suppressed the growth of NF90.8, sNF96.2 and ST88–14 cells, compared to the EGFP construct as control (Fig. 1C).

Next, we compared the transduction efficacy of a panel of commercially available AAV vectors in MPNST and primary human Schwann cells by expressing EGFP and quantifying the green fluorescent signals. We used 13 hybrid pAAV-Rep-Cap (pAAV-RC) vectors, which encode the rep of AAV2 and variable *cap* genes of different serotypes, including AAV1 (pAAV2/1), AAV2 (pAAV2-RC), AAV3B (pAAV-RC3B), AAV4 (pAAV-RC4), AAV5 (pAAV2/5 JC), AAV6 (pAAV-RC6), AAV7 (pAAV2/7), AAV8 (pAAV2/8), AAV9 (pAAV9n), AAV10 (pAAV2/rh10), AAV11 (pAAV2/hu11) and AAV32/33 (pAAV2/rh32.33) as well as the synthetic AAV-DJ (pAAV-DJ) [24–27] [28], along with the pHelper and self-complimentary pscAAV (pscAAV-MCS) expression vector to enhance the transduction [29]. The pscAAV vector uses the CMV promoter to express the transgene. After production, purification and quantification of AAVs, 5000 ST88–14, NF90–8 or sNF96.2 cells were plated in 96-well plates and incubated with indicated AAVs at MOI 1000 or 5000. Cells were allowed to grow five days to reach complete confluence as examined optically by microscope. Green fluorescent signals in each well were quantified by a plate reader, which reflected the expression levels of EGFP in the transduced cells. At an MOI of 5000, AAV2,

3B and DJ demonstrated superior transduction of EGFP in ST88–14 cells, while in NF90–8 cells, AAV1, 2, 3B, 6 and DJ showed significant transduction in contrast to other AAVs (Fig. 2A and C). Cells incubated at MOI of 1000 followed a similar trend. The results were consistent with the observation of the fluorescence microscopy, where all the cells were photographed and either selectively shown in Fig. 2B and D or not shown. In sNF96.2 cells, AAV1, 2, 3B and DJ again stood out both at MOI 5000 and 1000 (Fig. 3A and B). Using flow cytometry, we measured in average 98.7% and 99.1% NF90–8 cells were positive of EGFP at MOI 1000 and 5000 of AAV-DJ-EGFP, respectively, with higher expression levels observed at MOI 5000 (Supplementary Fig. 1).

It has been established that neurofibromastosis 1 and MPNST are originated from Schwann cells [2, 30]. A gene replacement therapy restoring NF1 functions could also benefit the patients before the malignant transformation in *NF1* haploid cells, most importantly the Schwann cells. We transduced primary human Schwann cells (HSC) that are positive of S-100 staining (Fig. 3C) with 13 AAV vectors encoding EGFP and found AAV 1, 2, 6 and DJ delivered EGFP most efficaciously (Fig. 3D and E).

Next, we tested GRD constructs with AAV-DJ, one of the relatively efficacious AAV vectors consistently among MPNST and HSC. Because RAS proteins are attached to the cellular membrane through prenylation and palmitoylation of cysteine residues including a CAAX motif located in the C-terminal hypervariable region (HVR) that is sufficient to confer targeting to plasma membrane [31–33], we created a GRD construct fused with the 10 amino acids of H-Ras C-terminus (C10) containing the palmitoylation sites and CAAX motif, with a double HA tag at the N-terminus. When transduced by AAV-DJ in NF90–8 cells, GRD-C10 drastically outperformed GRD in suppressing the phosphorylation of Erk1/2 (pErk1/2) where a reduced pERK1/2 signal with GRD and no pErk1/2 signal with GRD-C10 was detected, while GRD-C10 showed a relatively low expression level in those cells (Fig. 4A). Using intracellular anti-HA staining and flow cytometry, we found that in average 13.2% and 9.8% NF90–8 cells were stained positive 36 hrs after transfected by AAV-DJ-GRD and AAV-DJ-GRD-C10 at MOI 5000, respectively (Supplementary Fig. 2). Immunofluorescence staining of HA demonstrated the membrane-targeting of GRD-C10 (Fig. 4B). GRD-C10 markedly outperformed GRD in suppressing the growth of ST88–14, NF90–8 and sNF96.2 cells (Fig. 4C–E). Cell cycle analysis of NF90–8 and ST88–14 cells indicated significantly less cells in G2/M phase and more cells in Sub-G0 48 hours after transduced with AAV-DJ-GRD-C10 compared to those with the control AAV-DJ (Fig. 4F and G, Suppl. Fig. 3). In contrast, despite being transducible with AAV-DJ (Fig. 5A and B), STS26C cells, a spontaneous MPNST cell line with intact NF1 (Fig. 1A), were not affected by GRD and GRD-C10 (Fig. 5C). Similarly, HSCs was not suppressed by GRD at all and also not by GRD-C10 at a significant level (Fig. 5D).

Discussion

The major challenge facing therapies using AAVs is the poor efficacy in delivery, to which many efforts have been directed in modifying and optimizing the AAV *cap* gene [34]. For example, aiming to improve targeting and reduce anti-AAV immunity, recombinant AAV-DJ was created via DNA shuffling and immuno-selection from *cap* genes of 8 natural serotypes

and markedly outperformed all the parental AAV vectors in vitro [28]. Further engineering of AAV-DJ resulted in drastically improved delivery in various mice tissues [28, 35]. In this study, we analyzed the transduction efficacies of recombinant vectors distinct from each other only on capsids of 12 natural serotypes of human and monkey origins and the synthetic AAV-DJ, in various MPNST cells and HSC. The consensual AAV1, 2, 3B and DJ as well as AAV6 that transduced HSC and NF90–8 particularly efficiently, can be used in testing in vivo and included as templates in future engineering efforts to improve targeting in MPNST and HSC in vitro and further in vivo.

Although AAV has not been tested with MPNST cells in previous publications before, Hoyng et al. have reported transduction of primary human and rat Schwann cells with AAV serotypes 1–9 carrying GFP in culture and in nerve segments [36]. In that study, AAV2 and AAV6 outperformed other vectors in cultured HSC, which is largely consistent with our finding in Fig. 3D.

NF1 is a large protein with various domains of complex functionalities, including cysteine serine-rich domain (CSRD), tubulin-binding domain (TBD), GRD, Sec14, PH-like domain and FAK-binding region [37]. A GRD version of 333 amino acids (AA) (NF1–333, AA 1198–1530) has been extensively investigated, which revealed a central minimal GAP domain of 230 AA (AA 1248–1477) and flanking extra regions that also appeared to mediate important GAP-related functions and interactions [37–39]. In physiological conditions, NF1 protein is recruited to the plasma membrane by interacting with Spred1, which has been mapped between Spred1 EVH1 domain and GRD's N- (AA 1202–1217) and C-terminal (AA 1511–1530) extra regions [40–42]. In this study, we used a slightly larger GRD sequence (AA 1172–1538) in our construct with a double HA tag [18]. This construct presented a diffused subcellular distribution in MPNST cells upon viral transduction. The C-terminal HVRs of Ras proteins with the CAAX motif contain cysteine residues subject to prenylation and palmitoylation that confer the targeting to the plasma membrane. For example, the C-terminal 11 AA, 10 AA, and 20 AA of respective N-Ras, H-Ras and K-Ras4B have been shown to re-target an exogenously expressed protein to the plasma membrane [31, 33]. In order to improve the targeting on membrane-associated Ras proteins, GRD was fused with an H-Ras C10 sequence containing cysteine 181 and 184 as well as the CAAX motif. This GRD-C10 construct drastically enhanced GRD's potency in suppressing pErk1/2 and the growth of NF1-related MPNST cells, with remarkable specificity as shown in contrast to NF1-unrelated MPNST cells and HSC. Thus, given its potency and specificity, GRD-C10 would be well suited in a gene replacement therapy in MPNST and *NF1*-haploid individuals in future development. In such a therapy, a noticeable efficacy would entail almost all of the MPNST cells or the majority of the *NF1*-haploid Schwann cells to receive the GRD-C10 transgene, since the non-transduced populations exhibit a clear growth advantage. With the current available tools for in vivo gene delivery, this would be only feasible with a drastically improved AAV vector for MPNST or Schwann cells, which could possibly be achieved through protein engineering of the AAV capsids. We further reason that a gene replacement therapy may have a good chance of success as a preventative measure before the malignant transformation to MPNST occurs by repeatedly targeting *NF1*-haploid Schwann cells that grow less aggressively than MPNST cells. Alternatively, approaches to upregulate the expression of *NF1* on the intact allele in *NF1*-haploid cells can also be

considered, for example via techniques with specific recognition such as CRISPR-dCas9-VPR, where the nuclease-null Cas9 is fused with a tripartite activator, VP64-p65-Rta (VPR) [43]. However, although the latter approach could produce more copies of the full-length NF1, it will also face acute limitations in the cloning capacity and transduction efficiency of AAV vectors.

Supplementary Material

Refer to Web version on PubMed Central for supplementary material.

Acknowledgements

We thank Mr. Richard (Lee) Blosser of BKI flow center for his valuable help in flow cytometry. This work was supported by Francis S. Collins Scholar Program (V.S.), 1K08CA230179–01 (V.S.), DHART-SPORE IN4689861JHU (V.S.), Children's Tumor Foundation 2016A-05–008 (V.S.), 1R03CA178118–01A1 (R.Y.B.), DOD W81XWH1810236 (R.Y.B.).

References

1. Carey JC, Baty BJ, Johnson JP, Morrison T, Skolnick M, Kivlin J. The genetic aspects of neurofibromatosis. Ann N Y Acad Sci 1986;486: 45–56. [PubMed: 3105404]
2. Staedtke V, Bai RY, Blakeley JO. Cancer of the Peripheral Nerve in Neurofibromatosis Type 1. Neurotherapeutics 2017;14: 298–306. [PubMed: 28349408]
3. Abramowicz A, Gos M. Neurofibromin in neurofibromatosis type 1 - mutations in NF1gene as a cause of disease. Dev Period Med 2014;18: 297–306. [PubMed: 25182393]
4. Ratner N, Miller SJ. A RASopathy gene commonly mutated in cancer: the neurofibromatosis type 1 tumour suppressor. Nat Rev Cancer 2015;15: 290–301. [PubMed: 25877329]
5. Mautner VF, Asuagbor FA, Dombi E, Funsterer C, Kluwe L, Wenzel R et al. Assessment of benign tumor burden by whole-body MRI in patients with neurofibromatosis 1. Neuro Oncol 2008;10: 593–8. [PubMed: 18559970]
6. De Raedt T, Beert E, Pasmant E, Luscan A, Brems H, Ortonne N et al. PRC2 loss amplifies Ras-driven transcription and confers sensitivity to BRD4-based therapies. Nature 2014;514: 247–51. [PubMed: 25119042]
7. Rodriguez FJ, Folpe AL, Giannini C, Perry A. Pathology of peripheral nerve sheath tumors: diagnostic overview and update on selected diagnostic problems. Acta Neuropathol 2012;123: 295–319. [PubMed: 22327363]
8. Zou C, Smith KD, Liu J, Lahat G, Myers S, Wang WL et al. Clinical, pathological, and molecular variables predictive of malignant peripheral nerve sheath tumor outcome. Ann Surg 2009;249: 1014–22. [PubMed: 19474676]
9. Evans DG, Baser ME, McGaughran J, Sharif S, Howard E, Moran A. Malignant peripheral nerve sheath tumours in neurofibromatosis 1. J Med Genet 2002;39: 311–4. [PubMed: 12011145]
10. Nathwani AC, Davidoff AM, Tuddenham EGD. Advances in Gene Therapy for Hemophilia. Hum Gene Ther 2017;28: 1004–1012. [PubMed: 28835123]
11. Guggino WB, Cebotaru L. Adeno-Associated Virus (AAV) gene therapy for cystic fibrosis: current barriers and recent developments. Expert Opin Biol Ther 2017;17: 1265–1273. [PubMed: 28657358]
12. Deverman BE, Ravina BM, Bankiewicz KS, Paul SM, Sah DWY. Gene therapy for neurological disorders: progress and prospects. Nat Rev Drug Discov 2018;17: 641–659. [PubMed: 30093643]
13. Lisowski L, Tay SS, Alexander IE. Adeno-associated virus serotypes for gene therapeutics. Curr Opin Pharmacol 2015;24: 59–67. [PubMed: 26291407]
14. Kotterman MA, Schaffer DV. Engineering adeno-associated viruses for clinical gene therapy. Nat Rev Genet 2014;15: 445–51. [PubMed: 24840552]
15. Naldini L Gene therapy returns to centre stage. Nature 2015;526: 351–60. [PubMed: 26469046]

16. Hiatt KK, Ingram DA, Zhang Y, Bollag G, Clapp DW. Neurofibromin GTPase-activating protein-related domains restore normal growth in Nf1−/− cells. J Biol Chem 2001;276: 7240–5. [PubMed: 11080503]
17. Dasgupta B, Gutmann DH. Neurofibromin regulates neural stem cell proliferation, survival, and astroglial differentiation in vitro and in vivo. J Neurosci 2005;25: 5584–94. [PubMed: 15944386]
18. Morcos P, Thapar N, Tusneem N, Stacey D, Tamanoi F. Identification of neurofibromin mutants that exhibit allele specificity or increased Ras affinity resulting in suppression of activated ras alleles. Mol Cell Biol 1996;16: 2496–503. [PubMed: 8628317]
19. Bai RY, Staedtke V, Aprhys CM, Gallia GL, Riggins GJ. Antiparasitic mebendazole shows survival benefit in 2 preclinical models of glioblastoma multiforme. Neuro Oncol 2011;13: 974–82. [PubMed: 21764822]
20. Bai RY, Dieter P, Peschel C, Morris SW, Duyster J. Nucleophosmin-anaplastic lymphoma kinase of large-cell anaplastic lymphoma is a constitutively active tyrosine kinase that utilizes phospholipase C-gamma to mediate its mitogenicity. Mol Cell Biol 1998;18: 6951–61. [PubMed: 9819383]
21. Bodempudi V, Yamoutpoor F, Pan W, Dudek AZ, Esfandyari T, Piedra M et al. Ral overactivation in malignant peripheral nerve sheath tumors. Mol Cell Biol 2009;29: 3964–74. [PubMed: 19414599]
22. Reuss DE, Mucha J, Hagenlocher C, Ehemann V, Kluwe L, Mautner V et al. Sensitivity of malignant peripheral nerve sheath tumor cells to TRAIL is augmented by loss of NF1 through modulation of MYC/MAD and is potentiated by curcumin through induction of ROS. PLoS One 2013;8: e57152. [PubMed: 23437333]
23. Sun D, Tainsky MA, Haddad R. Oncogene Mutation Survey in MPNST Cell Lines Enhances the Dominant Role of Hyperactive Ras in NF1 Associated Pro-Survival and Malignancy. Transl Oncogenomics 2012;5: 1–7. [PubMed: 22346343]
24. Gao GP, Alvira MR, Wang L, Calcedo R, Johnston J, Wilson JM. Novel adeno-associated viruses from rhesus monkeys as vectors for human gene therapy. Proc Natl Acad Sci U S A 2002;99: 11854–9. [PubMed: 12192090]
25. Cearley CN, Wolfe JH. Transduction characteristics of adeno-associated virus vectors expressing cap serotypes 7, 8, 9, and Rh10 in the mouse brain. Mol Ther 2006;13: 528–37. [PubMed: 16413228]
26. Cearley CN, Vandenberghe LH, Parente MK, Carnish ER, Wilson JM, Wolfe JH. Expanded repertoire of AAV vector serotypes mediate unique patterns of transduction in mouse brain. Mol Ther 2008;16: 1710–8. [PubMed: 18714307]
27. Mays LE, Wilson JM. Identification of the murine AAVrh32.33 capsid-specific CD8+ T cell epitopes. J Gene Med 2009;11: 1095–102. [PubMed: 19777488]
28. Grimm D, Lee JS, Wang L, Desai T, Akache B, Storm TA et al. In vitro and in vivo gene therapy vector evolution via multispecies interbreeding and retargeting of adeno-associated viruses. J Virol 2008;82: 5887–911. [PubMed: 18400866]
29. Wang Z, Ma HI, Li J, Sun L, Zhang J, Xiao X. Rapid and highly efficient transduction by double-stranded adeno-associated virus vectors in vitro and in vivo. Gene Ther 2003;10: 2105–11. [PubMed: 14625564]
30. Zhu Y, Ghosh P, Charnay P, Burns DK, Parada LF. Neurofibromas in NF1: Schwann cell origin and role of tumor environment. Science 2002;296: 920–2. [PubMed: 11988578]
31. Hancock JF, Cadwallader K, Paterson H, Marshall CJ. A CAAX or a CAAL motif and a second signal are sufficient for plasma membrane targeting of ras proteins. EMBO J 1991;10: 4033–9. [PubMed: 1756714]
32. Simanshu DK, Nissley DV, McCormick F. RAS Proteins and Their Regulators in Human Disease. Cell 2017;170: 17–33. [PubMed: 28666118]
33. Choy E, Chiu VK, Silletti J, Feoktistov M, Morimoto T, Michaelson D et al. Endomembrane trafficking of ras: the CAAX motif targets proteins to the ER and Golgi. Cell 1999;98: 69–80. [PubMed: 10412982]
34. Weinmann J, Grimm D. Next-generation AAV vectors for clinical use: an ever-accelerating race. Virus Genes 2017;53: 707–713. [PubMed: 28762205]

35. Mao Y, Wang X, Yan R, Hu W, Li A, Wang S et al. Single point mutation in adeno-associated viral vectors -DJ capsid leads to improvement for gene delivery in vivo. BMC Biotechnol 2016;16: 1. [PubMed: 26729248]

36. Hoyng SA, De Winter F, Gnavi S, van Egmond L, Attwell CL, Tannemaat MR et al. Gene delivery to rat and human Schwann cells and nerve segments: a comparison of AAV 1–9 and lentiviral vectors. Gene Ther 2015;22: 767–80. [PubMed: 25938190]

37. Scheffzek K, Shivalingaiah G. Ras-Specific GTPase-Activating Proteins-Structures, Mechanisms, and Interactions. Cold Spring Harb Perspect Med 2018.

38. Ahmadian MR, Wiesmuller L, Lautwein A, Bischoff FR, Wittinghofer A. Structural differences in the minimal catalytic domains of the GTPase-activating proteins p120GAP and neurofibromin. J Biol Chem 1996;271: 16409–15. [PubMed: 8663212]

39. Scheffzek K, Ahmadian MR, Wiesmuller L, Kabsch W, Stege P, Schmitz F et al. Structural analysis of the GAP-related domain from neurofibromin and its implications. EMBO J 1998;17: 4313–27. [PubMed: 9687500]

40. Stowe IB, Mercado EL, Stowe TR, Bell EL, Oses-Prieto JA, Hernandez H et al. A shared molecular mechanism underlies the human rasopathies Legius syndrome and Neurofibromatosis-1. Genes Dev 2012;26: 1421–6. [PubMed: 22751498]

41. Hirata Y, Brems H, Suzuki M, Kanamori M, Okada M, Morita R et al. Interaction between a Domain of the Negative Regulator of the Ras-ERK Pathway, SPRED1 Protein, and the GTPase-activating Protein-related Domain of Neurofibromin Is Implicated in Legius Syndrome and Neurofibromatosis Type 1. J Biol Chem 2016;291: 3124–34. [PubMed: 26635368]

42. Dunzendorfer-Matt T, Mercado EL, Maly K, McCormick F, Scheffzek K. The neurofibromin recruitment factor Spred1 binds to the GAP related domain without affecting Ras inactivation. Proc Natl Acad Sci U S A 2016;113: 7497–502. [PubMed: 27313208]

43. Chavez A, Scheiman J, Vora S, Pruitt BW, Tuttle M, E PRI et al. Highly efficient Cas9-mediated transcriptional programming. Nat Methods 2015;12: 326–8. [PubMed: 25730490]

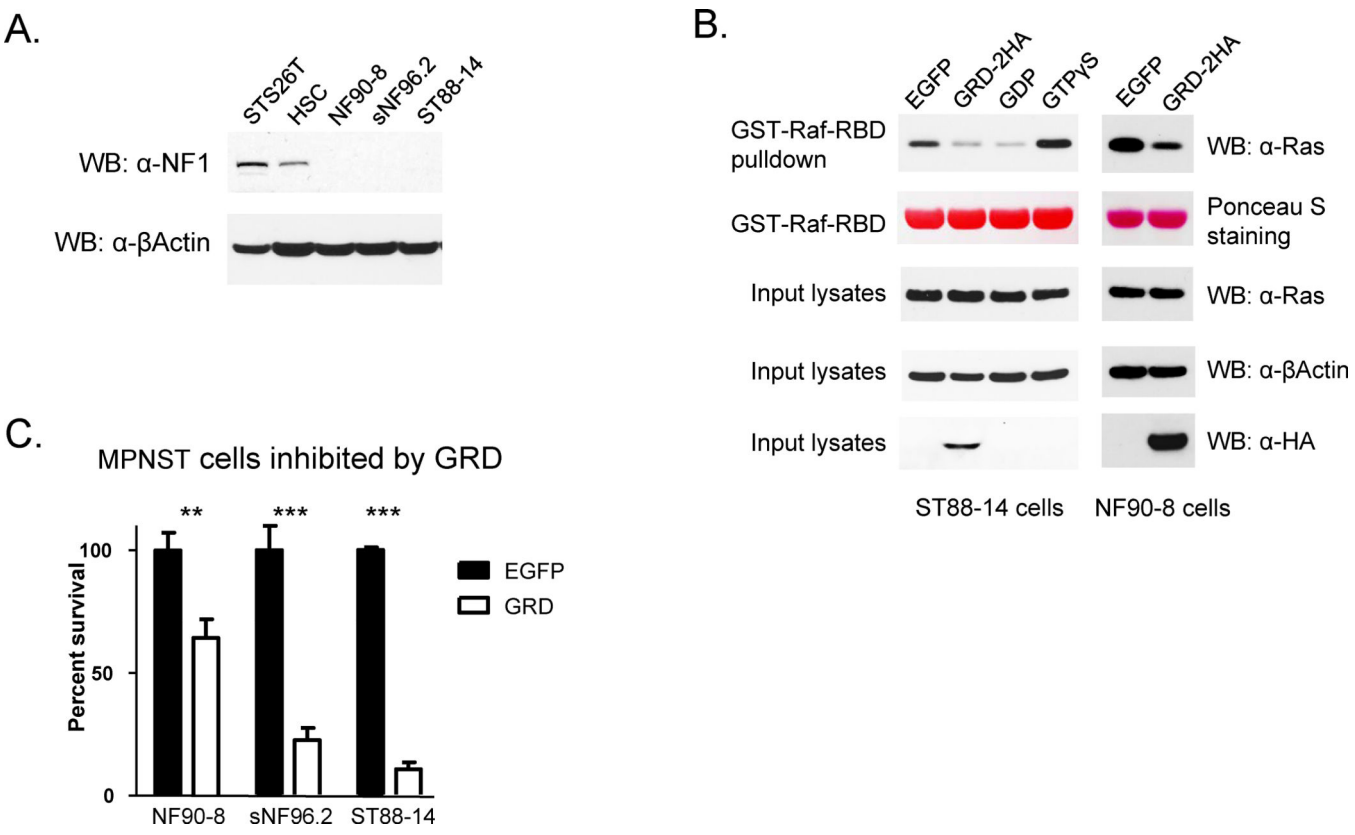

Figure 1. Overexpression of GRD suppressed MPNST cells

A. NF1 expression in MPNST cells. Western blotting was performed with the lysates of NF1-related MPNST cells (NF90–8, sNF96.2 and ST88–14), NF1-unrelated MPNST STS26T, and human Schwann cells (HSC).

B. Overexpression of NF1-GRD reduced Ras activities in MPNST cells. ST88–14 and NF90–8 were transduced by EGFP or GRD-2HA lentivirus and cell lysates were subjected to pulldown assay with GST-Raf-RBD. Western blotting was performed with indicated antibodies. GTPγS and GDP represent the positive or negative control, respectively.

C. NF1-GRD suppressed the growth of MPNST cells. MPNST cells were transduced with EGFP or GRD-2HA via lentivirus in 96 well plates and viable cells were measured after 72 hrs. Three biological samples were measured in each date point and P values were evaluated by two-tailed t-test.

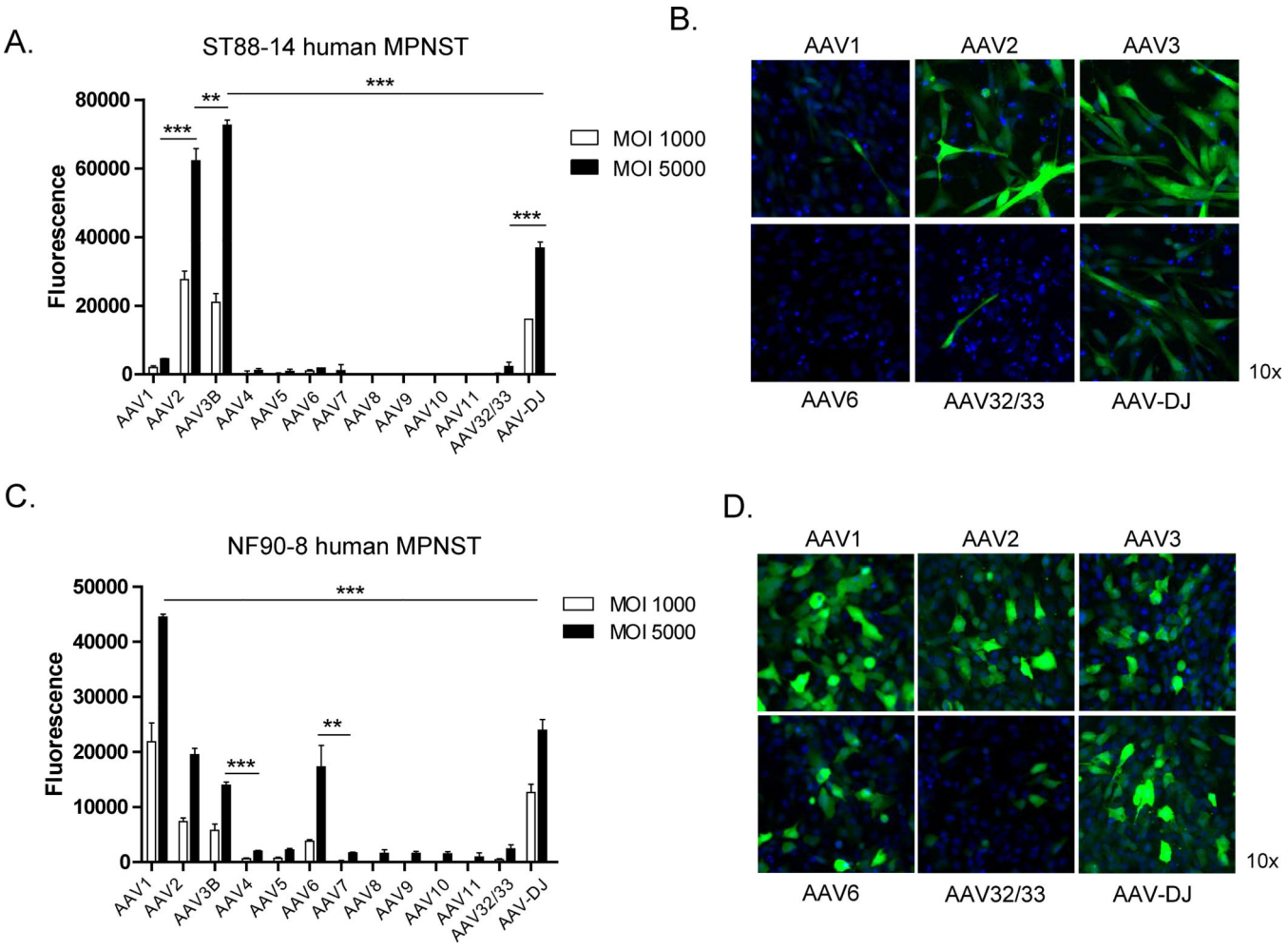

Figure 2. Transduction of EGFP with various AAVs in ST88–14 and NF90–8 cells

A. Transduction efficacies of different AAV vectors in ST88–14 cells. ST88–14 cells plated in 96 well plates were transduced with indicated AAVs at MOI 1000 or 5000. Green fluorescent signals were measured after 5 days. Three biological samples were measured in each data point and statistical significance was evaluated by two-tailed t-test.

B. Fluorescence images of EGFP in ST88–14 cells transduced by selected AAVs. Nuclei were stained by NucBlue Live Cell Stain in blue.

C. Transduction efficacies of different AAV vectors in NF90–8 cells. NF90–8 cells plated in 96 well plates were transduced with indicated AAVs at MOI 1000 or 5000. Green fluorescent signals were measured after 5 days.

D. Fluorescence images of EGFP in NF90–8 cells transduced by selected AAVs. Nuclei were stained by NucBlue Live Cell Stain in blue.

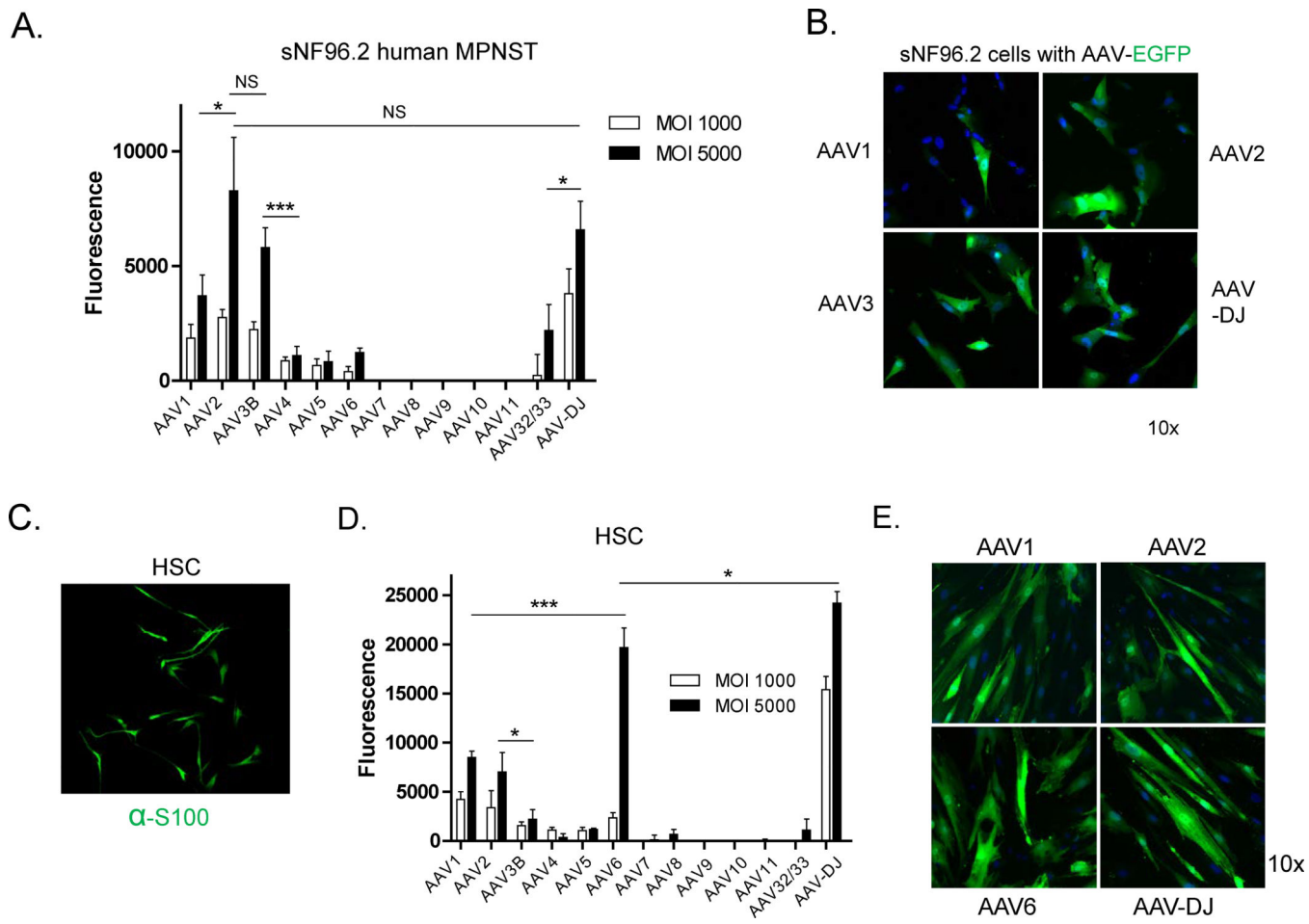

Figure 3. Transduction of EGFP with various AAVs in sNF96.2 and HSC cells

A. Transduction efficacies of different AAV vectors in sNF96.2 cells. sNF96.2 cells plated in 96 well plates were transduced with indicated AAVs at MOI 1000 or 5000. Green fluorescent signals were measured after 5 days. Three biological samples were measured in each data point and statistical significance was evaluated by two-tailed t-test.

B. Fluorescence images of EGFP in sNF96.2 cells transduced by selected AAVs. Nuclei were stained by NucBlue Live Cell Stain in blue.

C. Green fluorescence staining of human spinal nerve Schwann cells with anti-S100 antibody.

D. Transduction efficacies of different AAV vectors in human Schwann cells. HSC plated in 96 well plates were transduced with indicated AAVs at MOI 1000 or 5000. Green fluorescent signals were measured after 5 days.

E. Fluorescence images of EGFP in HSC transduced by selected AAVs. Nuclei were stained by NucBlue Live Cell Stain in blue.

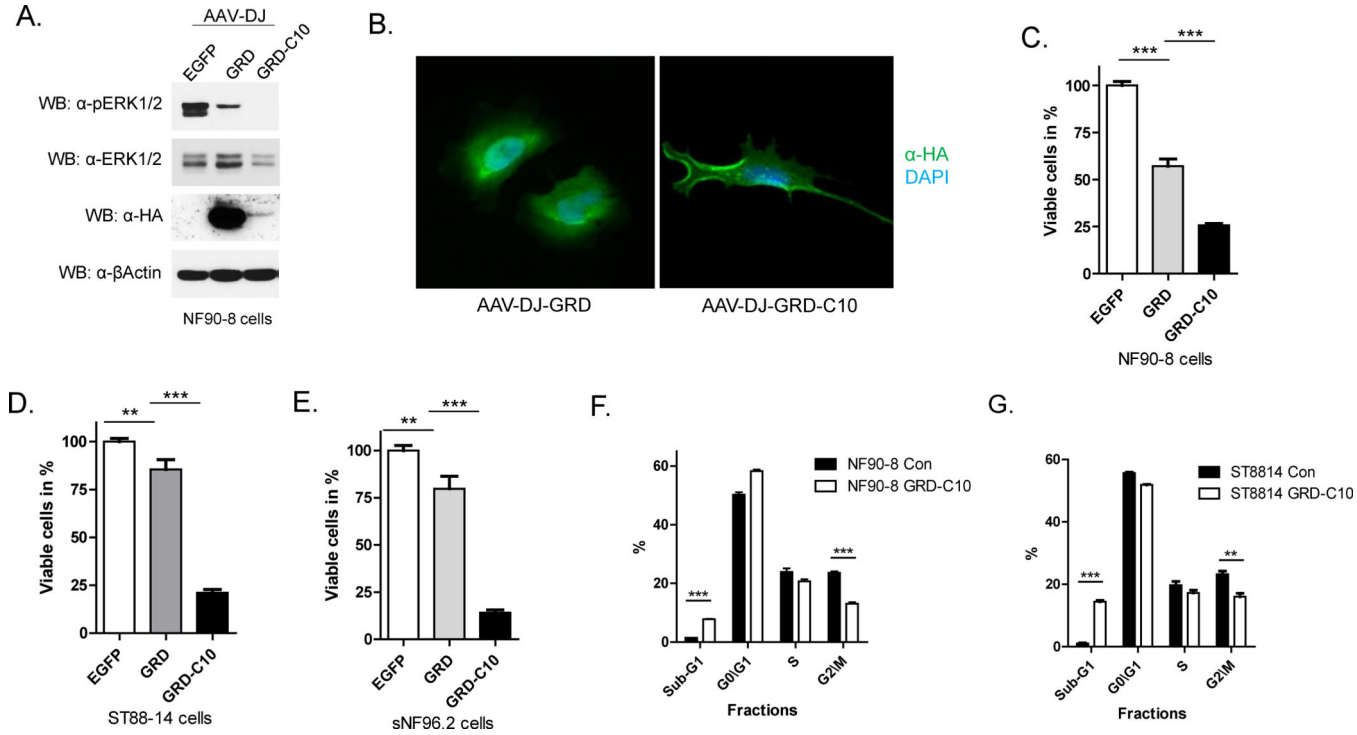

Figure 4. Suppression of MPNST cells by GRD and GRD-C10 transduced by AAV-DJ

A. Transduction of GRD-2HA and 2HA-GRD-C10 in NF90–8 cells by AAV-DJ. NF90–8 cells were transduced at MOI 5000 by AAV-DJ carrying EGFP (control), GRD-2HA or 2HA-GRD-C10. Anti-HA western blot showed the expression of GRD-2HA and 2HA-GRD-C10, and anti-pERK1/2 blot demonstrated the complete inhibition of ERK1/2 (p42/44) phosphorylation by GRD-C10 construct. Anti-ErK1/2 blot showed the total levels of Erk1/2 in the lysates, whereas anti-βActin was used as control of housekeeping gene.

B. Anti-HA immunofluorescence images of NF90–8 cells transduced with GRD-2HA or 2HA-GRD-C10 by AAV-DJ. Nuclei were stained by DAPI in blue.

C-E. Inhibition of MPNST cells by GRD and GRD-C10 transduced by AAV-DJ. NF90–8, ST88–14and sNF96.2 cells were plated in 96 well plates and incubated with AAV-DJ carrying EGFP, GRD-2HA or 2HA-GRD-C10 constructs at MOI 5000. After 4 days, viable cells were measured. Three biological samples were measured in each data point and P values were evaluated by two-tailed t-test.

F and G. NF90–8 and ST8814 cells were transduced by control AAV-DJ or AAV-DJ-2HA-GRD-C10 at MOI 5000. After 2 days, cells were harvested, stained by propidium iodide and analyzed by flow cytometry (n=3). Fractions were calculated and P values were evaluated by two-tailed t-test.

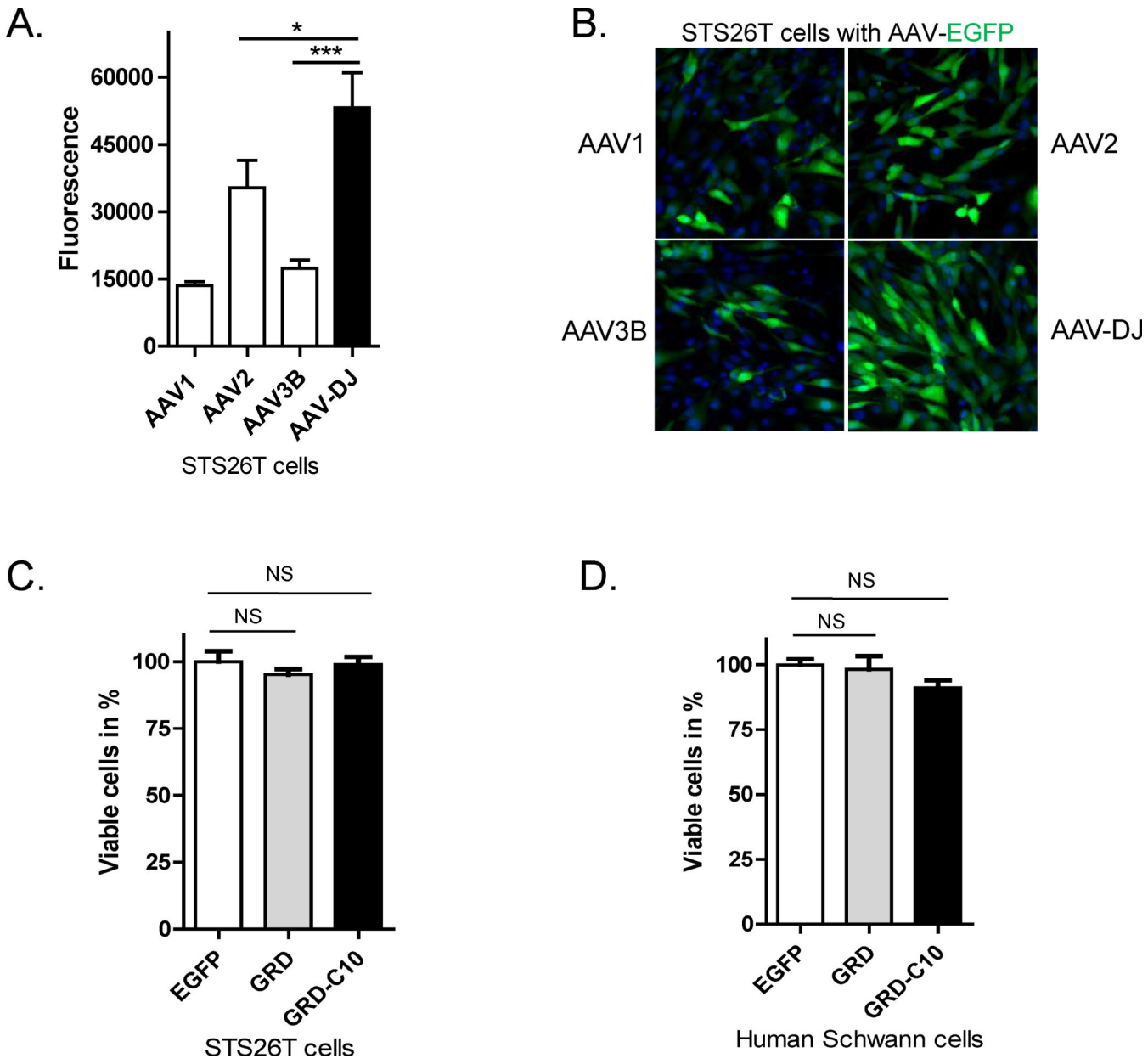

Figure 5. STS26 and human Schwann cells were not significantly affected by GRD and GRD-C10 transduced by AAV-DJ.

A. Transduction efficacies of different AAV vectors in STS26T cells. Cells plated in 96 well plates were transduced with indicated AAVs at MOI 5000. Green fluorescent signals were measured after 5 days. Three biological samples were measured in each data point and statistical significance was evaluated by two-tailed t-test.

B. Fluorescence images of EGFP in STS26T cells transduced by indicated AAVs. Nuclei were stained by NucBlue Live Cell Stain in blue.

C and D, STS26T MPNST cells and human Schwann cells were plated in 96 well plates and incubated with AAV-DJ carrying EGFP, GRD-2HA or 2HA-GRD-C10 constructs at MOI 5000. After 4 days, viable cells were measured. Three biological samples were measured in

each data point and statistical significance was evaluated by two-tailed t-test. NS: not significant, $p > 0.05$.